BRITTLE FRACTURE UNDER MIXED MODE I/MODE II LOADING

T.M. Maccagno* and J.F. Knott*

The brittle fracture of four different materials under mixed mode I/mode II loading has been investigated using precracked bend bar specimens loaded in anti-symmetric and symmetric four-point-bend configurations. The materials and test temperatures were: En3B mild steel at -196°C, En24 high strength steel at 20°C, PMMA at 20°C, and oolitic limestone at 20°C. The results are used to test and discuss two mixed mode fracture criteria. It is concluded that a maximum stress criterion holds for brittle material, but requires modification if non-linear flow at the crack tip precedes fracture.

INTRODUCTION

Fracture toughness evaluation for mode I (opening) loading is well-established. Flaws in real structures however, are rarely subjected to pure mode I alone. Generally, the loading will be some combination of mode I, mode II (shearing), and mode III (tearing), and it follows that design procedures based on mode I alone may be of limited usefulness when applied to loading conditions in service. The aim of the present work is to examine the conditions for mixed mode crack extension in engineering alloys and develop a general approach to characterize such fracture.

Previous research into crack extension in combined modes I, II, and III loading has employed a number of different loading configurations, but for mixed mode I/mode II fracture toughness testing, the anti-symmetric four-point-bend arrangement (AS4PB) devised by Gao et al (1) appears to be particularly straightforward to use. This loading arrangement is shown in Figure 1,

*Department of Metallurgy and Materials Science
University of Cambridge

together with the associated shear force and bending moment diagrams. It is readily applied to conventional bend bar specimens which can be sharply cracked by pre-fatiguing in the normal way.

With reference to Figure 1, mode II is associated with the shear force Q and mode I is associated with the bending moment M, so that the relative amount of mode II to mode I loading K_{II}/K_I varies with crack position along the bar. At the centre of the bar, no M exists yet there is a substantial Q, so the applied stress state is pure mode II and K_{II}/K_I is very large. As the crack is positioned further from the centre, more M is introduced and K_{II}/K_I decreases. In order to obtain pure I conditions use is made of the symmetric four-point-bend arrangement (S4PB) for which pure bending (i.e. Q = 0) conditions exist in the central region of the specimen. The symmetric arrangement is also shown in Figure 1, together with the associated shear force and bending moment diagrams. It is clear that by using the AS4PB and changing the crack position, and by using the S4PB, a wide range from pure mode II to pure mode I may be obtained.

The values for the crack tip stress intensity factors K_I and and K_{II} for a specimen of width W and thickness B may be determined from (2).

$$K_I = \frac{M}{BW^{3/2}} f_b\left(\frac{a}{w}\right) \qquad \ldots\ldots (1)$$

$$K_{II} = \frac{Q}{BW^{1/2}} f_s\left(\frac{a}{w}\right) \qquad \ldots\ldots (2)$$

where $f_b(\frac{a}{w})$ and $f_s(\frac{a}{w})$ are the calibration functions for pure bending and pure shear given in Table 1.

In order to demonstrate that the AS4PB does indeed give mixed mode I and II crack tip loadings by simple alteration of the crack position, a birefringence investigation was carried out on a photoelastic material (polycarbonate), which exhibits stress-induced birefringence under polarized light. The patterns produced by various mode II to mode I stress ratios may be examined to determine whether the forms of the stress/strain fields are consistent with what would be expected. Figure 2 shows that the birefringence patterns produced around the crack tip for different crack positions are consistent with what would be expected in changing from pure mode I to pure mode II, and these observations correlate well with other analytical, numerical and photoelastic studies (3,4,5). The angle β, used in the captions to Figure 2, is explained later with reference to Figure 4.

TABLE 1 - Calibration functions for bend bars

$(\frac{a}{w})$	$f_b(\frac{a}{w})$	$f_s(\frac{a}{w})$
0.20	4.97	0.496
0.25	5.67	0.667
0.30	6.45	0.857
0.35	7.32	1.080
0.40	8.35	1.317
0.45	9.60	1.557
0.50	11.12	1.838
0.55	13.09	2.125
0.60	15.66	2.441

EXPERIMENTAL

The materials used in this investigation were selected in accordance with the following criteria. The first point was that all the materials selected should fracture in a catastrophic brittle manner which could be approximated as "linear elastic" behaviour, in the hope that Irwin's (6) analytical description of the stress field near a crack tip (in terms of $\sigma_\theta, \tau_r, \tau_{r\theta}$) would then be applicable. In addition to the ability to fracture in an overall brittle manner however, it was also planned that each material should separate by a different micro-mechanism of fracture.

Finally, it was desired that the mechanical and physical properties should be sufficiently well established so as to eliminate extraneous uncertainties in the interpretation of results.

On the basis of these criteria, the materials chosen to be tested were two steels (En3B, En24), a glassy polymer (PMMA), and a building stone (oolitic limestone).

Normalized En3B is a typical mild steel and fractures by a "transgranular cleavage" mechanism at cryogenic temperatures. Quenched and tempered En24 is a high strength steel which

macroscopically cracks normal to the mode I stress, but fails by what is microstructurally a "fast shear" mechanism at room temperature, although this is sufficiently catastrophic to give a valid K_{IC} result. PMMA is a glassy polymer which is thought to fail in a brittle manner by rapid formation and separation of a single craze at the tip of an advancing crack. Oolitic limestone (oolite) is composed of spherical grains of calcite (approx. 0.5mm diameter) bonded together by a dense calcareous cement, and fractures by debonding of the cement under stress. Oolite is not a common engineering material when subjected to tensile loads, but it was selected because it fractures in an "ideally brittle" manner, whereas steel and PMMA, even under so-called "brittle" conditions, develop limited but possibly significant non-linear benaviour at the crack tip prior to the actual fracture event. Details of the conventional mechanical properties for the four materials are given in Table 2.

TABLE 2 - Conventional mechanical properties.

Material	Temperature (^{o}C)	Tensile Yield Stress (MPa)	Ultimate Tensile Stress (MPa)	Elongation (%)	E (GPa)	Poisson's ratio ν
En3B	-196	840	880	25.9	205	0.3
En24	20	1380	2160	15.7	205	0.3
PMMA	20	-	60	-	2	0.4
Oolite	20	-	5	-	50	0.25

Specimens of En3B 10mm thick x 20mm wide x 80mm long were fractured in a 250 kN capacity MAND servo-hydraulic testing machine at a test temperature of -196^{o}C. Specimens of En24 with identical dimensions to those of En3B were tested in the same machine but at +20^{o}C. The cross head displacement rate for both sets of tests was 0.5 mm/min. The specimens of PMMA measured 5 x 20 x 80mm and were tested at +20^{o}C in a screw-driven Hounsfield tensometer of 2.5 kN capacity, and at a cross head displacement of 6mm/min. The oolite specimens measured 20 x 20 x 80mm and were tested in a screw-driven INSTRON machine of 5000 kg capacity and at a cross head displacement of 0.2mm/min.

RESULTS

The mixed mode I and II testing using the AS4PB and S4PB arrangements resulted in all specimens fracturing in a brittle manner. For all four materials, the introduction of mode II causes the crack to extend catastrophically at an angle θ_o to the original crack plane, and this angle θ_o generally increases with increasing mode II component. This phenomenon is apparent in Figure 3 which shows mixed mode specimens of En24 fracture at 20°C. The fracture angle θ_o was measured for each specimen, and the applied load at fracture P_f was used in equations (1) and (2) to calculate the mode I stress intensity factor at fracture K_{If} and the mode II stress intensity factor at fracture K_{IIf}.

These experimental values of θ_o for all specimens are plotted against the relative amount of mode I and mode II applied to the crack tip prior to fracture in Figure 4. Note that in this figure the abscissa, representing the relative amount mode I to mode II, is given in terms of the corresponding angle β in a centre-cracked plate subjected to uniaxial tension. Also plotted on this figure is the manner in which the plane of maximum resolved tensile stress at the crack tip $\sigma_{\theta max}$ varies with the relative amounts of mode I to mode II. This relation is obtained by differentiating Irwin's expressions for σ_θ (under combined tensile and shear loads) and then setting the result equal to zero to calculate the value of θ_o. It can be seen that the experimental points appear to correspond reasonably well with the plane of maximum σ_θ, with the results for the oolite, PMMA, and En24 steel appearing to follow the theoretical line quite closely.

Scanning Electron Microscopy of the fracture surfaces of En24 and of En3B revealed that there were no significant differences between the fracture surfaces of cracks that had been initially loaded in a stress field composed of a shearing component (mode II) and those that had been initially loaded in a pure mode I stress field. Figure 5 compares the fracture surfaces of En3B tested at -196°C which, prior to fracture, were subjected to a pure mode I applied stress field and a pure mode II applied stress field. The fracture surfaces of the oolite and PMMA specimens were observed under the optical microscope, and once again, there were no differences between the specimens loaded in pure applied mode I and specimens loaded in mixed modes I and II or pure applied mode II.

DISCUSSION

In the case of pure applied mode I, crack propagation in brittle materials is thought to be tensile stress controlled, and may be described in terms of a critical stress criterion in which the local tensile stress must exceed some critical value over a microstructurally significant distance (7). Observation of the fracture surfaces indicate that for the materials tested, the mechanisms of crack extension in mixed modes I and II are identical to those in pure mode I. It seems reasonable to suppose then that the angle of brittle crack extension θ_o for a crack initially subjected to a mixed mode I and II stress field should be the plane normal to which the resolved tensile stress σ_θ is maximum. This seems well-supported by the results shown in Figure 4.

The hypothesis that brittle fracture in mixed modes I and II loading is controlled by the maximum σ_θ was first tested by Erdogan and Sih (8) in an investigation using PMMA panels containing central cracks at an angle β to the applied normal load, in order to obtain mixtures of mode I and mode II. They proposed that the angle of fracture θ_o is the direction for which σ_θ is a maximum, and that the fracture initiates when $\sigma_{\theta max}$ reaches a constant critical value unique to the material. Using Irwin's expressions for crack tip stress fields, such a criterion may be stated as:

$$\sigma_{\theta Cr} = \frac{K_{If}}{(2\pi r)^{\frac{1}{2}}} \cos^3 \frac{\theta_o}{2} - \frac{K_{IIf}}{(2\pi r)^{\frac{1}{2}}} 3 \sin \frac{\theta_o}{2} \cos \frac{\theta_o}{2} \quad \ldots\ldots (3)$$

where K_{If}, K_{IIf} and θ_o have their previous definitions. It is possible to check this hypothesis by simply substituting the values of K_{If}, K_{IIf}, and θ_o found in the present work to determine whether $\sigma_{\theta Cr}$ remains constant as the applied load combination varies from pure mode I to pure mode II. Figure 6 shows the results of this exercise when carried out for oolite and PMMA. Note that the ordinate of the graph is normalized in both cases by dividing the value of $\sigma_{\theta Cr}$ at $\beta = 90^o$ (i.e. mode I). It appears that $\sigma_{\theta Cr}$ for oolite remains approximately constant throughout the range from mode I to mode II, but that $\sigma_{\theta Cr}$ for PMMA does not. The results for En3B and En24 are similar to PMMA in that they do not remain constant. This is an extremely important point. It appears then, that for an ideally brittle material (i.e. oolite), for which there is no non-linear flow at the crack tip prior to fracture, the fracture under mixed modes I and II is well described by a maximum σ_θ criterion incorporating Irwin's elastic expressions for the crack tip stress field. However, materials which do develop non-linearity at the crack tip prior to fracture (i.e. PMMA, steel) do not appear to be described very well by such a maximum σ_θ criterion, although observations of the fracture

surfaces of the PMMA and steel specimens suggest that brittle fracture of these materials in mixed modes I and II is tensile stress controlled. One possibility is that the crack tip stress fields for such materials are not well described by Irwin's expressions, and this points to the need for development of realistic elastic/plastic crack tip stress and strain fields under mixed mode loading.

Another possible reason for the discrepancy between theory and experiment, in the case of materials that develop plasticity, and still consistent with a maximum σ_θ criterion, presents itself if the micromechanisms of the crack extension are considered. In the case of steels, it is thought that transgranular cleavage and fast shear are nucleated by dislocation pile-ups (9). It is possible that an increase in the dislocation density, by introducing a shear component to the loading, is likely, at a given value of K_I, to facilitate carbide cracking in the case of cleavage, or facilitate carbide-matrix decohesion in the case of fast shear. If the nucleation stage is of significance, this could have the effect of decreasing the characteristic distance over which the local tensile stress must be achieved, and this would, in turn, increase the local stress intensification and thus lower the applied stress (or applied K_I) required to produce a local stress equal to the critical stress. This suggestion, that the critical distance may be affected by the introduction of a mode II component to the loading, again cannot be tested properly until appropriate stress analyses are available.

The suggestion that mixed modes I and II brittle may be described by a strain energy criterion has also been investigated in this work. According to Irwin (6) the strain energy release rate G in mixed modes I and II is given by:

$$G = \frac{(1-\nu^2)}{E} (K_I^2 + K_{II}^2) \qquad \text{.....(4)}$$

where E is Young's modulus and ν is Poisson's ratio for the material. The argument then supposes that failure initiates when some critical value G_{Cr}, which is constant and unique to the material, is attained. Once again this criterion may be checked by substituting the values of K_{If} and K_{IIf} found in the present work and then observing whether or not the calculated G_{Cr} remains constant throughout the range from mode I to mode II. The results for oolite and PMMA are plotted in Figure 7 and it may be seen that G_{Cr} does <u>not</u> remain constant for either of these two materials. Once again note that the ordinate is normalized by the value of G_{Cr} at $\beta = 90^o$. The results for En3B and En24 also do not suggest a constant G_{Cr}. The conclusion is that strain energy is not controlling the mixed mode I and II brittle fracture behaviour of the

four materials tested, and from equation (4), it may also be deduced that such fracture is not characterized by a critical value of K_{eff}, defined as:

$$K_{eff} = (K_I^2 + K_{II}^2)^{\frac{1}{2}} \quad \ldots\ldots\ldots (5)$$

CONCLUSIONS

(1) The combination of using anti-symmetric and symmetric four-point-bend arrangements is convenient and easily applied to study of mixed modes I and II fracture.

(2) For very brittle materials, such as oolite, mixed mode I and II fracture occurs along the plane of maximum resolved tensile stress when a constant critical value $\sigma_{\theta crit}$ is attained.

(3) For materials that develop significant non-linear behaviour at the crack tip prior to fracture, such as steel and PMMA, observation of the fracture surfaces and of the fracture angles suggests that crack extension in mixed modes I and II also occurs along the plane of maximum resolved tensile stress. The actual stress at failure however, is complicated by the fact that local crack tip non-linearity is associated with the fracture process, and this points to the need for the development of realistic/elastic plastic crack tip stress and strain fields under mixed mode loading.

ACKNOWLEDGEMENTS

The support for one of the authors (TMM) by the Edmonton Churchill Scholarship Foundation is gratefully acknowledged. Thanks are also due to Dr. G. Green of the C.E.G.B. Southwestern Region Laboratories for his support and contributions to this project. The authors also wish to thank Professor D. Hull for provision of research facilities.

SYMBOLS USED

a = crack length (m)

P_f = load applied to specimen at fracture (N)

Q = shear force (N)

M = bending moment (Nm)

B = thickness of bend bar (m)

W = width of bend bar (m)

K_{If} = mode I stress intensity factor at fracture (MPa$\sqrt{m}$)

K_{IIf} = mode II stress intensity factor at fracture (MPa$\sqrt{m}$)

$f_b(\frac{a}{w})$ = mode I calibration function

$f_s(\frac{a}{w})$ = mode II calibration function

E = Young's modulus (GPa)

ν = Poisson's ratio

θ_o = fracture angle (deg)

$\sigma_{\theta max}$ = maximum resolved tensile stress at crack tip (MPa)

$\sigma_{\theta Cr}$ = critical value of $\sigma_{\theta max}$ when fracture intiates (MPa)

G_{Cr} = strain energy release rate at fracture

REFERENCES

(1) Gao Hua et al., Acta Metallurgica Sinica, 15, 1979, pp. 380-391.

(2) Wang Ke Jen et al., "Calculation of stress intensity factors for combined mode bend specimens", in ICF4-Fracture 1977, Vol. 4, Waterloo, 1977, pp. 123-133.

(3) Sanford, R.J. and Dally, J.W., Engineering Fracture Mechanics, 11, 1979, pp. 621-633.

(4) Chisholm, D.B. and Jones, D.L., Experimental Mechanics, 17, 1977, pp. 7-13.

(5) Gao Hua and Chang Shao-ti, Acta Metallurgica Sinica, 12, 1981, pp. 1-15.

(6) Irwin, G.R., Journal of Applied Mechanics, 24, 1957, pp. 361-364.

(7) Ritchie, R.O. et al., Journal of the Mechanics and Physics of Solids, 21, 1973, pp. 395-410.

(8) Erdogan, F. and Sih, G.C., Journal of Basic Engineering, Transactions ASME, 85, Series D, 1963, pp. 519-527.

(9) Knott, J.F., "Micromechanisms of fracture and fracture toughness of engineering alloys", in ICF4-Fracture 1977, Vol. 1, Waterloo, 1977, pp. 61-92.

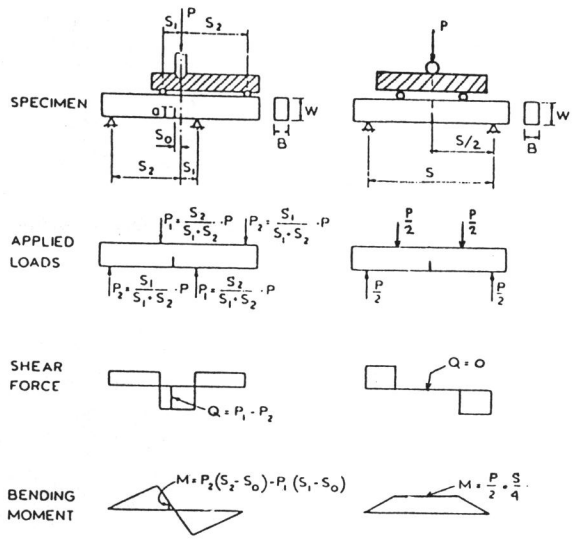

Figure 1 Antisymmetric and symmetric four-point-bend configurations.

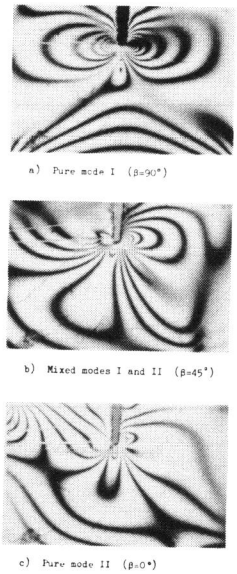

Figure 2 Birefringence patterns for four-point bend.

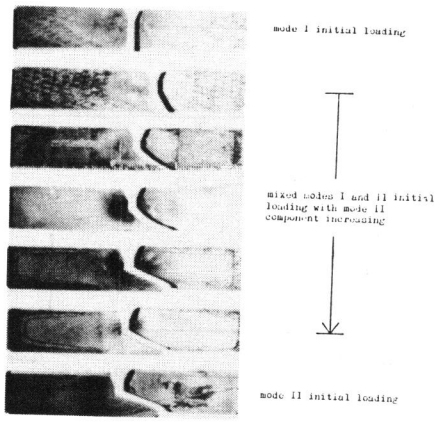

Figure 3 Mixed mode specimens of En24 tested at 20°C.

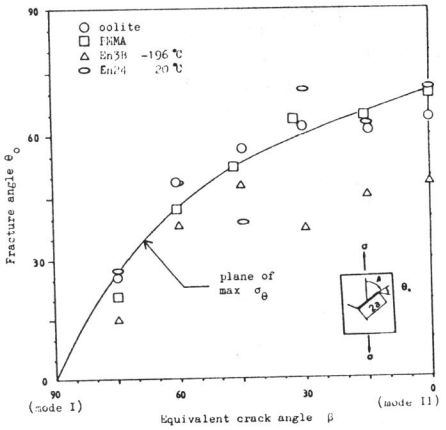

Fig. 4 Fracture angle θ_o vs relative amount of mode I and mode II.

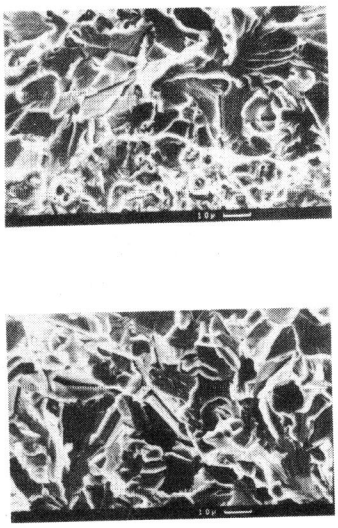

Fig. 5 Fracture surfaces of En3B tested at -196°C.

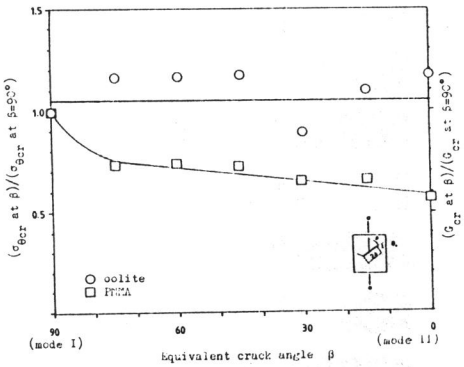

Fig. 6 $\sigma_{\theta Cr}$ vs relative amount of mode I to mode II.

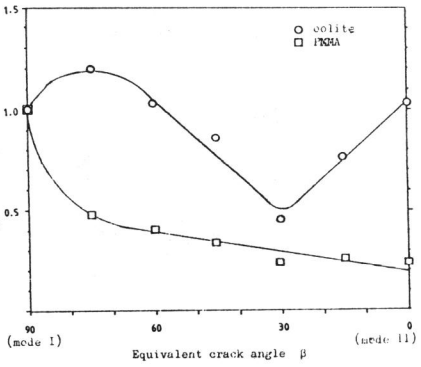

Fig. 7 G_{Cr} vs relative amount of mode I to mode II.